Comparison of kinetic Monte Carlo and molecular dynamics simulations of diffusion in a model glass former

Thomas F. Middleton and David J. Wales
University Chemical Laboratories, Lensfield Road, Cambridge CB2 1EW, United Kingdom

(Received 25 September 2003; accepted 4 February 2004)

We present results from kinetic Monte Carlo (KMC) simulations of diffusion in a model glass former. We find that the diffusion constants obtained from KMC simulations have Arrhenius temperature dependence, while the correct behavior, obtained from molecular dynamics simulations, can be super-Arrhenius. We conclude that the discrepancy is due to undersampling of higher-lying local minima in the KMC runs. We suggest that the relevant connectivity of minima on the potential energy surface is proportional to the energy density of the local minima, which determines the ''inherent structure entropy.'' The changing connectivity with potential energy may produce a correlation between dynamics and thermodynamics. © *2004 American Institute of Physics.* [DOI: 10.1063/1.1690241]

I. INTRODUCTION

Many liquids fail to crystallize on cooling below their freezing points and exist in a metastable supercooled state instead. On further cooling a glass transition temperature T_g is reached, at which the system exhibits the mechanical properties of a solid, while retaining the microscopic disorder of the liquid state. Supercooled liquids exhibit a variety of anomalous properties. Among the most interesting and widely studied is the tendency of transport properties to slow down more rapidly on approaching the glass transition than the Arrhenius law $\exp(-\Delta G^{\dagger}/RT)$ would predict. The effective activation free energies for these processes, $\Delta G^{\dagger}$, appear to increase as the temperature decreases. Di Marzio and Yang have pointed out that a number of functional forms appear to fit the experimental data reasonably well, because they are ''...three-parameter fits and the curves [are] rather structureless to begin with.''[1] The Vogel–Tammann–Fulcher (VTF) equation is probably the most commonly used functional form:[2–4]

$$\tau = \tau_0 \exp[A/(T-T_0)], \tag{1}$$

where τ is the relaxation time, A is a constant, and T_0 is a nonzero temperature, at which the relaxation time appears to diverge. The VTF expression is usually a good fit over two to four orders of magnitude in relaxation time in the temperature range approaching the glass transition.[5,6] The viscosity η may also be fitted to this form.

Angell has used plots of $\ln \eta$ against T_g/T to classify supercooled liquids as ''strong'' or ''fragile.''[7] Those at the strong extreme, for which the activation energy is temperature independent, tend to be covalent network formers, of which the most familiar example is probably SiO_2. A strength parameter D_T is sometimes defined as $D_T = A/T_0$. Here D_T diverges for strong liquids, because $T_0 = 0$ for materials that obey the Arrhenius law exactly. An analogous equation can be used to describe the pressure dependence, with a similarly defined strength parameter D_P (Refs. 8 and 9).

It is reasonable to assume that the dominant process limiting transport and relaxation in SiO_2 is the breaking of the Si–O bond. However, the interactions in fragile liquids tend to be weaker and less directional, involving Coulomb or van der Waals forces. In fragile liquids, the transition from glass to liquid is often marked by a large jump in the heat capacity, a feature that Angell has associated with a higher energy density of local minima on the potential energy surface (PES) and low barriers separating them.[10] The discontinuity in the heat capacity has been used to define a ''thermodynamic fragility,'' but it is important to note that the appearance of the heat capacity peak depends on the experimental cooling rate and does not correspond to equilibrium data. Liquids exhibiting super-Arrhenius dynamical behavior are usually found to be thermodynamically fragile, and this nontrivial correlation between kinetics and thermodynamics has prompted much discussion.

Liquids have higher specific heats than crystals, and so the entropy difference between the liquid and crystal decreases as the liquid is cooled. Kauzmann pointed out[11] that extrapolation of experimental data for the excess entropy implies that it would vanish for many liquids at a nonzero temperature T_K. If this trend were continued below T_K, the entropy of the liquid would fall below that of the crystal. Such an ''entropy crisis'' would violate the third law of thermodynamics. In practice, however, the glass transition intervenes, rapidly decreasing the heat capacity to a value similar to that of the crystal. Kauzmann's paradox is that the glass transition, a kinetic phenomenon when observed experimentally, enables the system to avoid breaking a thermodynamic law.

Strong liquids tend to have relatively large values of T_K. Indeed, Angell has pointed out that T_K correlates well with the VTF divergence temperature T_0 and has suggested that $T_0 \equiv T_K$ and that this corresponds to the ''configurational ground-state temperature''[12]—i.e., the temperature at which the liquid would occupy the lowest potential energy amorphous minimum if it were cooled infinitely slowly in the

absence of crystallization. Under these conditions it has also been suggested that an ''ideal'' second-order glass transition would occur at T_K, following Gibbs and Di Marzio's theoretical studies.[13,14]

In the current work we attempted to simulate diffusion in a model glass former using the kinetic Monte Carlo (KMC) approach, assuming that the dynamics of the supercooled liquid can be described by jumps between local minima on the PES, mediated by true transition states with precisely one negative eigenvalue.[15] Our results exhibit systematic discrepancies compared to molecular dynamics simulations, but the reason for these departures may provide insight into how super-Arrhenius behavior arises from the structure of the PES. The paper is arranged as follows: in Sec. II we outline some relevant theories concerning super-Arrhenius dynamics, Sec. III deals with implementation of KMC simulations, and in Secs. IV and V we present and analyze our results.

II. SUPER-ARRHENIUS DYNAMICS AND ENTROPY

There are numerous theories that attempt to explain super-Arrhenius dynamics. Three that are particularly relevant to the present work are the Adam–Gibbs–Di Marzio approach,[13,14,16] random-energy and instantaneous normal-mode theories,[17–24] and Dzugutov's scaling law.[25]

A. Adam–Gibbs equation

Adam and Gibbs built on the entropic theories of Gibbs and Di Marzio,[13,14,16] deriving a relation between the relaxation time of the supercooled liquid and an entropy S_{IS}:

$$\tau = \tau_0 \exp\left(\frac{C\Delta\mu}{TS_{\mathrm{IS}}}\right), \tag{2}$$

where $\Delta\mu$ is the free energy barrier per molecule or polymer segment in the cooperative group, and C and A are constants. The derivation treats a polymer as a collection of independent subsystems, each composed of z monomers, which rearrange in a cooperative fashion. S_{IS} is usually interpreted as the ''inherent structure (IS) entropy,'' which results from the alternative local minima on the PES. The next assumption is that the free energy barrier to rearrangement in this cooperative region is proportional to z—i.e., equal to $z\Delta\mu$. While this approach seems reasonable for polymer glasses, in which relaxation takes place by the rotation of polymer segments, it is not obvious why it should apply for nonpolymeric or non-networking-forming glasses with low molecular weight, such as orthoterphenyl (OTP) or the binary Lennard-Jones (BLJ) model discussed later in this paper. Notwithstanding this criticism, the Adam–Gibbs equation has successfully fitted data obtained for various glass-forming systems.[26–39] Sastry's results for the binary Lennard-Jones model are of particular interest to us.[34] He obtained the configurational entropy using the relationship $S_{\mathrm{IS}} \approx S_{\mathrm{total}} - S_{\mathrm{vib}}$, where S_{vib} is the vibrational entropy within the harmonic approximation. The temperature and IS entropy dependence of the diffusivity predicted by the Adam–Gibbs approach, $\ln D \sim 1/TS_{\mathrm{IS}}$, provided a good fit to the simulation results. As shown above, the IS entropy must be proportional to $T - T_0$ if the Adam–Gibbs and VTF equations are to be consistent. Sastry found S_{IS} to be almost linear with $T - T_0$, with a slight increase in slope at lower temperatures.[34] The fact that the Adam–Gibbs equation may also reproduce the temperature dependence of the diffusion constant, even when the entropy difference between the liquid and crystal is used instead of S_{IS}, suggests that these two entropies may be linearly related as a function of temperature.[37]

B. Random-energy model and instantaneous normal modes

Random-energy models (REM's), first analyzed by Derrida,[40] are based upon the assumption of a Gaussian configurational density of states. The REM exhibits both an entropy crisis and super-Arrhenius temperature behavior for the typical escape time from a potential energy minimum, and in the mean-field limit it is mathematically equivalent to mode-coupling theories.[17] Derrida's original proof of the properties of the REM is somewhat involved:[40] a simpler derivation can be found in Wolynes' review.[17]

In the most straightforward case, the typical escape time is given by[17]

$$\tau = \tau_0 \exp[\Delta E^2/2(k_B T)^2]. \tag{3}$$

This equation was used by Ferry[41] to describe the viscosity of various liquids, although he subsequently improved his fit by using the VTF law in Eq. (1).

Random-energy models have also been related to theories of transport properties based on instantaneous normal modes (INM's).[18–24] The INM methodology builds on Zwanzig's theoretical relationship for the interminimum transition rate on the PES and self diffusion constant.[42] The instantaneous normal modes are the eigenvectors of the mass-weighted Hessian, whose eigenvalues are the squares of the instantaneous angular frequencies. These eigenvalues are averaged over an equilibrium distribution of configurations sampled in a molecular dynamics trajectory. At sufficiently high temperatures a significant fraction of the INM frequencies will be imaginary, corresponding to negative eigenvalues of the Hessian. INM theory employs a relationship between the fraction of imaginary frequencies, f_u, and the hopping rate between minima, ω_h. Remarkably, it appears that for many supercooled liquids $D \sim \langle f_u \rangle$. A problem in the application of the theory is that there are modes with imaginary frequencies caused by anharmonicity, and these do not contribute to diffusion. Partial minimization of the configurations appears to filter out most of these irrelevant modes.[43,44]

Adam and Gibbs originally used the ''configurational'' entropy S_c in their equation (2). S_c has subsequently been defined in several different ways and is sometimes identified with S_{IS}. In this paper, however, S_c is understood as the entropic contribution from the full configurational coordinate space, while S_{IS} is the entropy due to the number of different alternative minima and does not include vibration. A relationship between f_u and the configurational entropy S_c has recently been proposed,[45] and LaNave *et al.* have found a linear relationship between S_{IS} and $\ln f_{dw}$, the fraction of imaginary normal modes with double-well potential energy profiles.[46] Keyes has related these observations to the REM

described above,[24] by treating the states in the REM as an ensemble of minima and saddles. In this REM-INM model the definition of S_{IS} is extended to regions of the PES associated with stationary points of any index,[23,24] although it may not be straightforward to define such a mapping in practice.[47,48]

C. Universal scaling law for diffusion

Dzugutov has discovered a simple scaling law relating the diffusion constant to the difference in entropy between the liquid and equivalent ideal gas, S_{ex} (Ref. 25). The collision frequency derived from Enskog theory,[49,50] Γ_E, and the ''effective'' hard sphere diameter σ were used to define a dimensionless diffusion constant D^*:

$$D^* = D\Gamma_E^{-1}\sigma^{-2}, \tag{4}$$

where D is the diffusion constant. The collision rate in Enskog theory is given by $\Gamma_E = 4\sigma^2 g(\sigma)\rho\sqrt{\pi k_B T/m}$, where σ is the hard-sphere diameter, $g(\sigma)$ the magnitude of the radial distribution function (RDF) at the point of contact, ρ the number density, and m the mass. In practice σ and $g(\sigma)$ are taken as the position and magnitude of the first maximum in the RDF. Local structural relaxation was then assumed to be limited by the number of accessible configurations per atom, represented by $\exp(S_{ex})$. In the normal (not supercooled) liquid domain there appears to be a nearly universal law that $D^* = 0.049\exp(S_2)$, where S_2 is the excess entropy given by a two-body approximation.[51] This relationship even appears to be successful for diffusion of silver ions in solid AgI, where the cations are distributed randomly within a lattice of I^- ions. Agreement was not so good for silicon modeled by the Stillinger–Weber (SW) potential,[52] perhaps because of the strong directional element in the interatomic potential invalidating the use of the Enskog collision frequency.

In a recent paper, Dzugutov has further developed his entropy-based theories of transport processes, studying diffusion in a metastable liquid of hard spheres.[53] In the hard-sphere liquid the free energy barrier to diffusion is entirely entropic, and D is proportional to $\exp(\Delta S^\dagger)$, where $\Delta S^\dagger$ is the entropy barrier. At high packing fractions ($\phi > 0.5$), D deviates from the behavior predicted in Eq. (4), and Dzugutov has suggested that a qualitative change in the form of the free energy landscape occurs. At low density all the possible configurations are abundantly connected, and the hard spheres are able to move in an essentially independent manner. As the system is compressed, the diffusive motion of the hard spheres is coupled within a certain range, which leads to additional entropic barriers to diffusion. We will discuss these observations further in the last two sections.

III. KINETIC MONTE CARLO SIMULATION OF DIFFUSION

In the current work we have simulated diffusion in the popular binary Lennard-Jones system using a kinetic Monte Carlo approach, building on previous, more qualitative studies of the PES.[54–56] The aim is not necessarily to provide an alternative to conventional molecular dynamics (MD) or MC simulations. Searching for minima and transition states is still a computationally expensive exercise, and so MD simulations remain the method of choice in the moderately supercooled region. Instead, calculation of dynamical properties directly from features of the PES will enable us to understand whether the connectivity of the minima and the magnitudes of the potential energy barriers between them can reproduce the super-Arrhenius behavior observed in MD simulations.

A. Principles of KMC

KMC simulations use a different importance sampling criterion from conventional MC simulations, associating a time scale with each step, which allows dynamic properties to be obtained. Fichthorn and Weinberg[57] were the first to put KMC simulations on a firm theoretical footing. Using the theory of Poisson processes, they showed that both static and dynamic properties could be calculated using the MC method. For systems in which the transition probabilities may often be small, the most efficient method of propagating the trajectory is the n-fold algorithm of Bortz, Kalos, and Lebowitz.[58] This scheme accepts a move at every trial by defining the transition probabilities as follows:

$$w_{ji} = k_{ji} \Big/ \sum_{m=1}^{n} k_{mi}, \tag{5}$$

where k_{ji} is the rate constant from minimum i to minimum j, and there are n transitions from which to choose.

It is worth noting that although the rate constants k_{ij} satisfy the detailed balance criterion, the w_{ji} do not: $w_{ji}P_i^{eq} \neq w_{ij}P_j^{eq}$. The w_{ij} and w_{ji} refer to different waiting times, and when this is taken into account, the detailed balance relation for the k_{ij} is retrieved.

The expectation value of the residence time in minimum i is

$$\langle \tau_i \rangle = 1 \Big/ \sum_j k_{ji}. \tag{6}$$

For $\langle \tau_i \rangle$ to be exact we must obtain the rates for all the transition states connected to minimum i. Of course, even if we have the patience and computer time to search exhaustively, the accuracy of $\langle \tau_i \rangle$ is limited by the rate theory used for the k_{ij} and the assumption that the rate constants correspond to independent Poisson processes. In practice, a representative sample of transition states is deemed sufficient. In the present work we have used Rice–Ramsperger–Kassel–Marcus (RRKM) theory[59–61] to obtain the microcanonical rate constants for the interminimum transitions. We have used microcanonical rate constants so that our results are directly comparable to the corresponding MD runs.

There are two main approximations in our calculations of the rate constants and equilibrium occupation probabilities. First, we assume that the phase space hyperellipsoids associated with each minimum do not overlap and can therefore be summed independently.[62,63] Second, we assume that the PES around each minimum is well represented by the harmonic approximation. This second assumption might prove problematic, since some near-universal properties of glass formers, such as the low-temperature specific heat

anomalies that have been attributed to the boson peak and two-level systems, suggest that anharmonicity can be important.[64] However, Broderix *et al.* deduced that the harmonic approximation was reasonable below a temperature of about $1\ k_BT/\epsilon_{AA}$ (Ref. 65) for the present system from MD simulations. They found that the potential energy per atom of the minima sampled was approximated surprisingly well by $e-3k_BT/2$, where e is the total internal energy per atom, in agreement with the harmonic approximation and classical equipartition theory.

B. Implementation of KMC simulations "on the fly"

The KMC approach has usually been used to simulate spatially ordered systems, particularly diffusion, adsorption, or aggregation on surfaces.[66–69] The order inherent in such systems means that the barriers of interest can often be obtained or guessed before the KMC trajectory is generated. Finding the transition probabilities therefore only requires an analysis of the transitions that are possible from the current configuration; for example, in surface diffusion we must know which jumps are possible given the occupancy of the adsorption sites.

In the current situation we have to calculate the transition states for each minimum that we visit "on the fly." Two recent examples of such a technique, which has not been attempted very often, are those of Hernández-Rojas and Wales for the 80:20 binary Lennard-Jones mixture[56] and Henkelman and Jónsson,[70] who studied the growth of the Al (100) surface. Snurr *et al.* have previously used this approach to study diffusion of benzene in silicalite.[71]

The previous KMC study of a BLJ system[56] used a 60-atom supercell, with 20 transition-state searches for each minimum. Random configurations were used to initiate each run, and 10^4 KMC steps were considered. The mean energy of the local minima, their structure factors, and the number of minima visited in a given number of steps were analyzed, but no dynamic properties were obtained. The results were found to be broadly consistent with MD; of particular interest was the observation that the number of minima visited decreased sharply at around $k_BT\sim 0.45\epsilon_{AA}$, close to the critical temperature of mode-coupling theory obtained by fitting to the diffusion constant.[72–74]

A 60-atom system is perhaps a little small, and so there may be some unwanted finite-size effects. However, there are obvious advantages in considering a small system for these initial investigations. For example, the number of transition states directly connected to each minimum is expected to scale as $\mathcal{O}(N)$.[47,48] The separation between time scales for vibration and rearrangements between local minima is also likely to be largest for smaller systems.[75–78]

In Refs. 54 and 55 we found that our algorithms are efficient in locating rearrangements with low barriers, but diffusion appears to require higher barrier processes. If we do not obtain enough transition states at each minimum visited in the KMC trajectory, nondiffusive rearrangements with low barriers will be selected too often.

C. Improvements in PES searching algorithms

KMC calculations are more demanding of our PES searching algorithms than the simple collection of minima and transition states discussed in previous work.[54,55] The results will only reflect the true properties of the system if we locate sufficient transition states connected to each minimum to provide a realistic representation of the complete distribution.

We used a test set of ten randomly selected minima from MD trajectories to evaluate the relative performance of different searching parameters and techniques. The waiting time at each minimum, $\langle\tau_i\rangle=1/\Sigma_j k_{ji}$, was the principal criterion that we used to assess the performance of each method and parameter set. The full details of this investigation have been omitted for brevity.[79]

Transition states were located in the present work using a single-ended method based on hard-sphere moves[54] and a double-ended algorithm, which links a pair of minima via one or more transition states using the nudged elastic band (NEB) approach.[80,81] We performed 84 single-ended searches and 16 double-ended searches from each minimum. New minima were generated by perturbing the coordinates of the current minimum and optimizing, to obtain destinations for the double-ended searches. The size of the perturbation was adjusted dynamically, decreasing it by 5% every time a new minimum was found and increasing by the same amount every time the original minimum was obtained. The double-ended NEB algorithm[80] was deemed to have failed if 20 transition states were found, without any being connected to the original minimum. After these searches were complete, a move to a new minimum was selected using the *n*-fold algorithm of Bortz, Kalos, and Lebowitz.[58]

We carried out MD and KMC runs for the 60-atom binary Lennard-Jones system at number densities of $1.1\sigma_{AA}^{-3}$, $1.2\sigma_{AA}^{-3}$, and $1.3\sigma_{AA}^{-3}$ (Refs. 72 and 74–82). The system consists of 48 A atoms and 12 B atoms, with interaction parameters $\sigma_{AA}=1.0$, $\sigma_{AB}=0.8$, $\sigma_{BB}=0.88$, $\epsilon_{AA}=1.0$, $\epsilon_{AB}=1.5$, and $\epsilon_{BB}=0.5$. We used the Stoddard–Ford quadratic cutoff,[83] so that both the potential energy and its first derivative are continuous. We adjusted the energies at which the runs were performed so that the diffusion constants measured were in the range $-11<\ln D<-3$, where D is expressed in units of $\sigma_{AA}\epsilon_{AA}^{1/2}m^{-1/2}$ and m is the atomic mass. This range extends from the moderately supercooled region to close to the minimum diffusion constant that can be measured accurately on the time scale of computer simulations. We used the MD runs both for comparison with the KMC results and to generate starting configurations for them. The MD simulations consisted of three independent microcanonical cooling runs, each including up to 27 consecutive stages, where the total energy was held constant for 10^5 equilibration steps and followed by 10^6 steps for data collection. The final configuration was used as the starting configuration for the following run, with the total energy decreased by $10\epsilon_{AA}$ ($0.17\epsilon_{AA}$ per atom). A velocity Verlet[84] algorithm was used with a time step of $0.005(m\sigma_{AA}^2/\epsilon_{AA})^{1/2}$ (Ref. 84), giving a cooling rate of $3.0\times10^{-5}(\epsilon_{AA}^3/m\sigma_{AA}^2)^{1/2}$/atom. The final configurations from the MD runs were used as the starting configurations

TABLE I. Starting and finishing energies for the MD and KMC runs, all expressed in ϵ_{AA} per atom. The energies in the MD cooling runs were changed in steps of $0.17\epsilon_{AA}$, while the KMC runs were carried out at energy intervals of $0.33\epsilon_{AA}$.

	Starting energy (MD)	Finishing energy (MD)	Highest energy (KMC)	Lowest energy (KMC)
$\rho=1.1$	0.00	−4.83	−1.50	−3.50
$\rho=1.2$	1.17	−3.17	−1.17	−3.17
$\rho=1.3$	3.00	−3.00	0.00	−1.17

for the KMC simulations, which were spaced at total energies of $0.33\epsilon_{AA}$. Table I summarizes these calculations.

For both MD and KMC simulations the diffusion constant at each temperature was obtained by calculating the gradient of a plot of $R(t)^2$ versus t, using linear regression. For the KMC results the data points for the first 2000 steps were discarded; points obtained in this section of the trajectory are likely to contain large fluctuations, especially at low temperatures. The displacement $R(t)$ obtained from KMC simulations is the distance from the starting minimum to the current minimum, while that obtained from MD simulations also contains a vibrational contribution. In the long-time limit, this difference should be negligible.

IV. RESULTS

The principal quantities of interest in comparing KMC and MD trajectories are the diffusion constants, which we can use to assess fragility,[7,12] and the energies of the minima sampled during the trajectory, which we can use to verify that the alternative simulations are sampling the same regions of phase space.

A. Diffusion constants

Figures 1–3 are Arrhenius plots of $\ln D$ vs ϵ_{AA}/k_BT, comparing diffusion constants obtained from KMC and MD simulations. Table II contains the relative performance of several standard fitting functions for the MD data at $\rho=1.1\sigma_{AA}^{-3}$ and $1.2\sigma_{AA}^{-3}$.

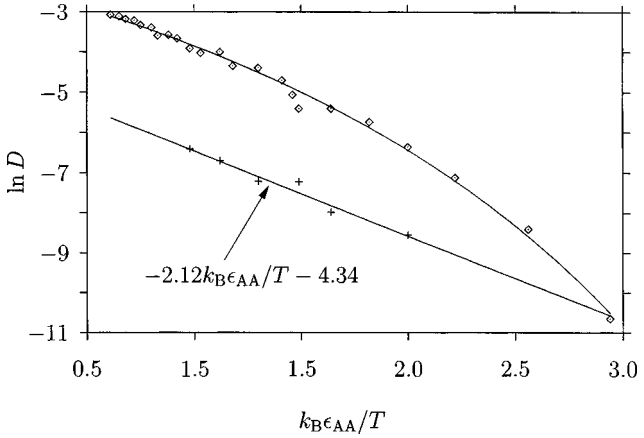

FIG. 1. Arrhenius plots of diffusion constants obtained from KMC (crosses) and MD (diamonds), at $\rho=1.1\sigma_{AA}^{-3}$. Included is the linear regression fit for the KMC diffusion constant, which indicates Arrhenius behavior.

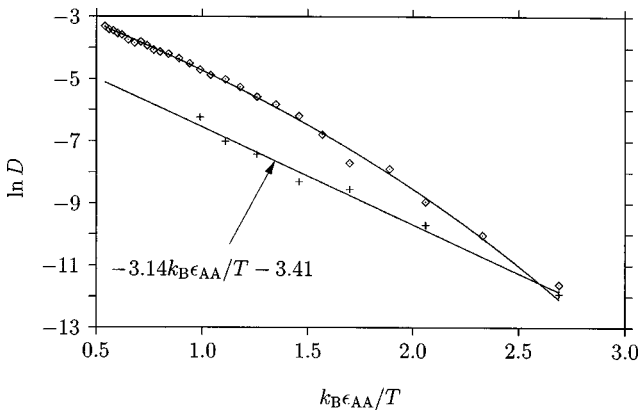

FIG. 2. Arrhenius plots of diffusion constants obtained from KMC (crosses) and MD (diamonds) at $\rho=1.2\sigma_{AA}^{-3}$. Included is the linear regression fit for the KMC diffusion constant, which again indicates Arrhenius behavior.

Several trends emerge as the density increases in the MD data. First of all, the linearity of the relationship between $\ln D$ and $1/T$ increases with ρ. The "strength parameter" A/T_0 lies in the range 8–9 for $\rho=1.1\sigma_{AA}^{-3}$ and 18–28 for $\rho=1.2\sigma_{AA}^{-3}$. Thus it appears that this system becomes *less fragile* with increasing density. These results appear to contradict Sastry's findings for a 256-atom system,[34] which suggested that the fragility increased with increasing density. Closer examination reveals that our parameters from VTF fits are similar to Sastry's at $\rho=1.1\sigma_{AA}^{-3}$: Sastry obtained $k_BT_0/\epsilon_{AA}=0.156$ and $A\sim1.2\epsilon_{AA}$ and we find $k_BT_0/\epsilon_{AA}=0.172$ and $A=1.41\epsilon_{AA}$. It appears that the smaller 60-atom system is subject to significant finite-size effects, especially at higher densities. However, as long as we take these into account when considering our results, they should not prevent us from drawing some preliminary conclusions about the nature of strong and fragile potential energy landscapes.

The KMC data are linear at all densities, with a similar activation energy to the limiting value for the MD data at high temperature, as judged from the gradient. The discrepancy increases with decreasing density: the diffusion constant from KMC simulations is smaller by factors of about 20 for $\rho=1.1\sigma_{AA}^{-3}$, about 10 for $\rho=1.2\sigma_{AA}^{-3}$, and about 3 for

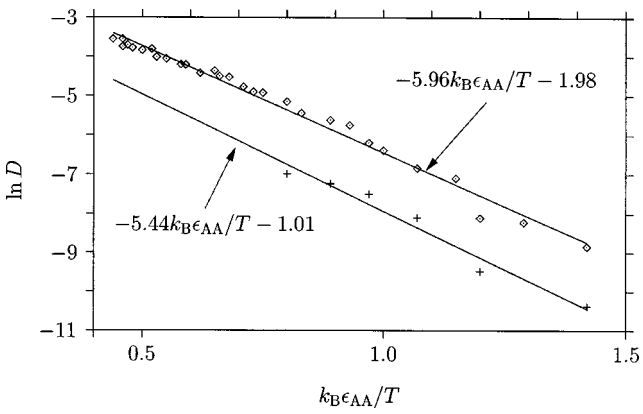

FIG. 3. Arrhenius plots of diffusion constants obtained from KMC (crosses) and MD (diamonds), at $\rho=1.3\sigma_{AA}^{-3}$. Both the KMC and MD results have been fitted using linear regression, as it appears that at this density the Arrhenius law is the most appropriate empirical fitting function.

TABLE II. Fits to the diffusion data obtained from MD simulations, with and without the point below $k_BT/\epsilon_{AA}=0.435$, which is usually taken as the mode-coupling critical temperature T_c (Refs. 72–74). The first fit is to the asymptotic MCT behavior $D\sim(T-T_c)^{\gamma}$, the second is to the VTF equation $D\sim\exp[A/k_B(T_0-T)]$, and the third is to a simple Arrhenius law $D\sim\exp(-\Delta E^{\dagger}/k_BT)$. The estimated variance V_{est} is included for each fit.

	$\rho=1.2\sigma_{AA}^{-3}$		
Parameter	Fits without $k_BT/\epsilon_{AA}=0.37$	Fits including $k_BT/\epsilon_{AA}=0.37$	$\rho=1.1\sigma_{AA}^{-3}$
k_BT_c/ϵ_{AA}	0.378±0.012	0.327±0.010	0.325±0.003
γ	2.159±0.124	2.520±0.137	1.757±0.062
V_{est}	0.045	0.072	0.032
A/ϵ_{AA}	2.428±0.022	2.738±0.177	1.408±0.088
T_0	0.133±0.021	0.097±0.016	0.172±0.010
V_{est}	0.018	0.021	0.020
$\Delta E^{\dagger}/\epsilon_{AA}$	3.810±0.080	3.710±0.091	2.903±0.120
V_{est}	0.041	0.047	0.124

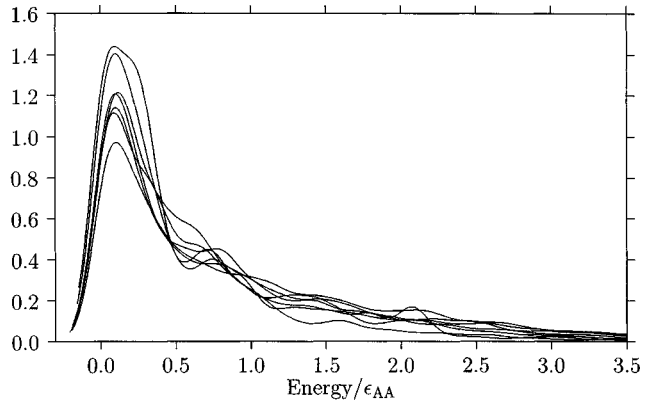

FIG. 4. Barrier distributions for accepted KMC moves at $\rho=1.2\sigma_{AA}^{-3}$. There is little significant difference between the samples, except that the size of the peak at low energy grows with decreasing temperature. The effective activation energy for diffusion obtained from an Arrhenius fit to the KMC results is $3.14\epsilon_{AA}$, which is considerably larger than the position of the principal maxima in the barrier distributions.

$\rho=1.3\sigma_{AA}^{-3}$ at the highest temperature. The data obtained from KMC simulations can also be fitted to the asymptotic MCT relationship $D\sim(T-T_c)^{\gamma}$. For simulations employing larger supercells and a shifted potential[73,74,85] it is accepted that $T_c\sim0.435$ at $\rho=1.2\sigma_{AA}^{-3}$, the number density for which most calculations have been performed. It is perhaps surprising that in the 60-atom system studied here, a measurable diffusion constant is obtainable below $k_BT/\epsilon_{AA}\sim0.4$. In part this must be due to the Stoddard–Ford truncation scheme and the cutoff of $1.842\sigma_{\alpha\beta}$, which decreases the well depth by 28% (Ref. 83).

We have quantified the degree to which the behavior of the 60-atom system is different from that observed in MD simulations with larger supercells.[72–74,85,86] In Table II we present the results from least-squares fitting using three different functions of $\ln D$ to $1/T$ for $\rho=1.1\sigma_{AA}^{-3}$ and $\rho=1.2\sigma_{AA}^{-3}$. The obvious functions to use are the asymptotic MCT relationship $D\sim(T-T_c)^{\gamma}$ and the VTF and Arrhenius equations. The MD data point at the lowest temperature, $k_BT=0.37\epsilon_{AA}$, has the greatest uncertainty and so we have included fits both with and without that point.

All the fitting parameters presented in Table II suggest that the system studied here is significantly different from one that uses a larger supercell.[72–74,85,86] At $\rho=1.2\sigma_{AA}^{-3}$, the mode-coupling critical temperature is lowered to between $0.32\epsilon_{AA}/k_B$ and $0.37\epsilon_{AA}/k_B$. This decrease is not altogether surprising, as it is similar in magnitude to the decrease in well depth compared to the standard Lennard-Jones potential. The value of the exponent γ is consistent with that obtained previously.[73] Of the three fitting functions, the VTF equation has the smallest estimated variance. T_0 is considerably lower than observed previously,[73] whether the lowest-temperature result is included or not. It is also worth noting that the estimated variance is of a similar order for all three fitting functions at number densities of $1.1\sigma_{AA}^{-3}$ and $1.2\sigma_{AA}^{-3}$.

For the densities that exhibit super-Arrhenius behavior, the coincidence of the mode-coupling critical temperature T_c and the point at which the two diffusion constants appear to merge is noteworthy. For $\rho=1.1\sigma_{AA}$ the value of T_c obtained from the least-squares fit is $0.35\epsilon_{AA}/k_B$, and the two fitted lines cross at $T=0.350\epsilon_{AA}/k_B$. For $\rho=1.2\sigma_{AA}$, these values are both around $0.38\epsilon_{AA}/k_B$. Thus it appears that the KMC and MD results agree around the critical temperature of MCT. This result is not entirely unexpected, for it is an accepted principle of MCT that as T_c is approached, so-called ''hopping'' processes become important, while the hydrodynamic-type diffusion modes become ''frozen out.'' These ''hopping'' or ''activated'' processes should be well described by the transition-state theory picture used here.

The activation energy in the KMC runs at density $1.2\sigma_{AA}^{-3}$, obtained from the Arrhenius plot (Fig. 2), is $-3.14\epsilon_{AA}$. If diffusion were a single-step process, we would expect to see barriers of this magnitude in the distribution function of barriers for accepted moves (Fig. 4). Unlike the previous distributions that we have published,[54,55] this distribution includes both uphill and downhill barriers, but only those accepted during the KMC run. Nevertheless, the results are very similar to the downhill distributions obtained in previous work,[54,55] spreading out slightly as the energy increases, when higher barrier moves are accepted more often. However, the negligible probability density at $E_{barrier}\sim3.14\epsilon_{AA}$ suggests that, as previously surmised, diffusion takes place by a multistage process, involving several transition states.

B. Energy distributions of local minima sampled

We quenched the MD configurations every 10^3 steps to generate a database of minima sampled by the cooling runs for comparison with the distributions obtained by KMC simulations. These distributions, visualized using the usual Gaussian method to produce smooth functions,[54] are presented in Fig. 5. For brevity, we have only included the distributions for number density $1.1\sigma_{AA}^{-3}$; these are qualitatively the same as those generated at the other two densities. The agreement between the distributions improves as the number density falls, and at low energies the distributions cover es-

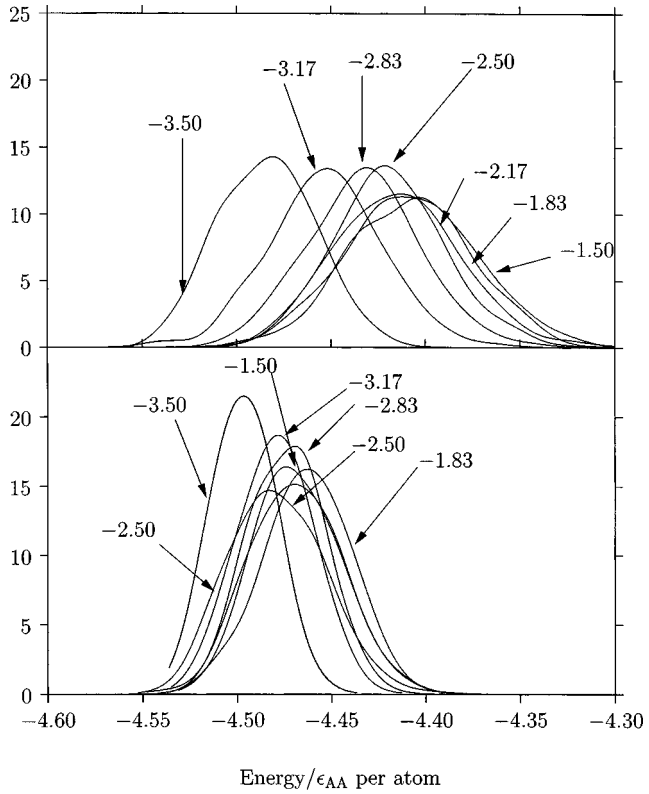

FIG. 5. Potential energy distributions of minima visited by MD (top panel) and KMC (bottom panel) simulations at $\rho=1.1\sigma_{AA}^{-3}$. The smooth distribution functions were generated using the Gaussian technique described in Ref. 54, with a width $s=0.01\epsilon_{AA}$. The total energies per atom at which the microcanonical MD and KMC runs were carried out are indicated in the figure. The agreement between MD and KMC simulations becomes increasingly good as the temperature decreases.

sentially the same energy range. These results are consistent with the trend in the discrepancies for the diffusion constant in the previous section.

The mean potential energies for the KMC runs at $\rho=1.2\sigma_{AA}^{-3}$ are shown in Table III; they follow the patterns of Fig. 5. The agreement with MD for the mean energies is good for the lowest three values, but becomes progressively worse as the total energy increases. It may be a concern that at higher energies, the microcanonical temperature is significantly higher for KMC simulations compared to the corresponding MD runs. We can obtain the harmonic microcanonical temperature from the density of states associated with a single minimum from the superposition approximation. Even for the highest temperature we get $k_BT/\epsilon_{AA}=1.12$, compared to the temperature in the corresponding MD run of $k_BT/\epsilon_{AA}=1.07$. Thus the discrepancy in the temperature is not very large, and we have used the same temperatures inferred from the MD runs in the Arrhenius plots for both the KMC and MD data.

TABLE III. Mean potential energies of the local minima sampled, $\langle v_{min}\rangle$, obtained from MD and KMC simulations at $\rho=1.2\sigma_{AA}^{-3}$ and at total energy per atom e_{tot}.

e_{tot}/ϵ_{AA}	$\langle v_{min}\rangle/\epsilon_{AA}$ (MD)	$\langle v_{min}\rangle/\epsilon_{AA}$ (KMC)
−1.17	−4.37	−4.43
−1.50	−4.39	−4.44
−1.83	−4.40	−4.45
−2.17	−4.42	−4.47
−2.50	−4.47	−4.48
−2.83	−4.49	−4.49
−3.17	−4.52	−4.51

TABLE IV. Maximum and minimum values of the ratio of the arithmetic mean waiting time in MD and KMC for each value of ρ. As the total energy is raised, the ratio increases approximately linearly for the two smaller number densities, but does not change much for $\rho=1.3\sigma_{AA}^{-3}$. The larger discrepancy between the two approaches for $\rho=1.1$ and $\rho=1.2\sigma_{AA}^{-3}$ with increasing energy is therefore unlikely to be caused by the harmonic approximation.

ρ/σ_{AA}^{-3}	Min$[\langle t_w^{KMC}\rangle/\langle t_w^{MD}\rangle]$	Max$[\langle t_w^{KMC}\rangle/\langle t_w^{MD}\rangle]$
1.1	2.67	9.95
1.2	0.95	5.62
1.3	1.75	4.67

The systematically lower potential energy obtained in the KMC runs may highlight sampling difficulties with KMC simulations, which appear to increase with increasing total energy. For the expected Gaussian probability distribution of potential energies for the local minima, there will generally be more minima at higher energy than lower energy connected to any given minimum in the range accessed by simulation. If our transition state searches find a higher proportion of the total connected minima at low energy, then a systematic bias will occur. The KMC diffusion constants may therefore correspond to a lower effective temperature, which would shift the values into better agreement with the MD results.

V. DISCUSSION

The discrepancies between KMC and MD simulations in both the diffusion constants and energies of the minima sampled are somewhat disappointing. However, the results are still interesting, as the differences in the KMC data may help us to elucidate the cause of the super-Arrhenius dynamics.

First of all, we have to question the principal assumptions in our implementation of the KMC algorithm in the present work. We have assumed that (1) populations of basins on the PES and transitions between them are well described using the harmonic superposition approximation,[62] (2) that the dynamics between basins are Markovian, and (3) that we have sampled phase space adequately. The validity of the harmonic approximation is supported by the results of Broderix *et al.*[65] Comparison of the waiting times for minima in KMC and MD runs—where we quenched at every step—are in Table IV. The KMC waiting times are obviously related to the sampling of the PES as well as the harmonic approximation. However, for number density $1.3\sigma_{AA}^{-3}$, the ratio of waiting times is only weakly temperature dependent, with an average value of 3.06 ± 1.18, which is very close to the discrepancy observed in the diffusion constant. Thus, in this case, where both MD and KMC results have an Arrhenius temperature dependence, the error in the prefactor can be accounted for entirely by the error in the waiting time. This

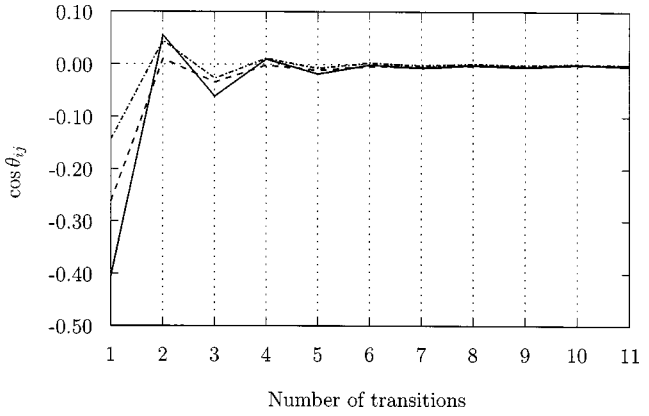

FIG. 6. Mean values of the cosine of the angle between successive transition vectors connecting local minima for the MD run at energy $-1.50\epsilon_{AA}$ and $\rho=1.1\sigma_{AA}^{-3}$. This is the MD run that has the greatest enhancement of the diffusion constant over the KMC run. The three lines represent (1) all interminimum transitions (solid line), (2) pure back correlations where $\cos\theta_{ij}=\pm1$ (dashed line), and (3) the difference between them (dot-dashed line). There is no positive correlation between successive transitions, suggesting that non-Markovian dynamics are probably not responsible for the super-Arrhenius behavior observed in the MD runs.

result probably has contributions from both sampling error and the harmonic approximation, but they appear to be relatively independent of the total energy. The results for the other two number densities therefore appear to be subject to an additional source of error, beyond that incurred by the harmonic approximation.

If the KMC diffusion constant were too small due to the breakdown of the Markovian assumption at high temperature, then there should be a positive correlation in the direction of successive transitions between minima. This question has been considered in depth by Keyes and Chowdhary (KC), who considered diffusion in a 32-atom Lennard-Jones system,[76] and Doliwa and Heuer (DH), who studied a 65-atom BLJ system.[87,88] Both groups found that any correlation present was entirely negative: for example, KC observed that removing the effect of correlation greatly enhanced the diffusion constant. DH coarse-grained the landscape into ''metabasins,'' which probably correspond to sets of local minima separated by relatively low barriers. We have previously referred to such structures as ''megabasins,''[54] and DH report that they observed weak backcorrelation for up to five intermegabasin transitions.

We can measure the directional nature of successive transitions between local minima by examining the cosine between the transition vectors leading to the ith and jth basins in a sequence, which can be obtained easily from the scalar product of the interminimum vectors:

$$\cos\theta_{ij}=\frac{(\mathbf{R}_i-\mathbf{R}_{i-1})\cdot(\mathbf{R}_j-\mathbf{R}_{j-1})}{|\mathbf{R}_i-\mathbf{R}_{i-1}||\mathbf{R}_j-\mathbf{R}_{j-1}|}, \tag{7}$$

where $\mathbf{R}_i$ is a $3N$-dimensional vector containing the coordinates of the ith minimum. In Fig. 6 we show the average value of this correlation function for $k_BT/\epsilon_{AA}=1$ and density $1.1\sigma_{AA}^{-3}$, where we expect to find the most positive correlation between successive transitions. Even the residue that remains after subtracting pure backcorrelations—i.e., those with $\cos\theta_{ij}=-1$—shows no significant positive correlation. Thus, on the basis of previous work[76,87,88] and the calculated directional correlation function, we conclude that the enhanced diffusion constant of the MD method over the KMC method is not due to non-Markovian behavior.

It therefore appears that the KMC runs have undersampled configuration space, as suggested by comparison of the distributions of minima discussed above. It is particularly interesting that the activation energy as measured by KMC simulations, $\Delta E_{KMC}^{\dagger}$, is much smaller than the limiting activation energy defined by the slope of the MD Arrhenius plot as $T\to T_c$, $\Delta E_{MD}^{\dagger}(T_c)$. If the super-Arrhenius behavior observed at number densities $1.2\sigma_{AA}^{-3}$ and $1.1\sigma_{AA}^{-3}$ were due to large potential energy barriers separating megabasins in the low-lying part of the PES, we would expect the limiting low-temperature activation energy to be the same for both KMC and MD simulations. In fact, $\Delta E_{KMC}^{\dagger}$ is much closer to the parameter A in the numerator of the exponential term in the VTF equation, which also corresponds to the activation energy when $T\gg T_0$. This result suggests that the potential energy barrier to diffusion is very similar for the low- and high-energy regions of the PES. Because the KMC sampling of higher-energy minima is relatively poor, there is no significant change in the prefactor for the KMC runs. The change in KMC rate with temperature is therefore energetic, with little entropic contribution. The origin of the super-Arrhenius behavior observed in MD therefore appears to be entropic and contained in the prefactor. This result does not necessarily contradict the findings of DH,[87,88] who found that the barriers between metabasins decreased with increasing potential energy. Over the temperature range that we consider, $k_BT/\epsilon_{AA}<1$, DH found that the temperature behavior of the diffusion constant is close to Arrhenius, implying that the rate-limiting energetic barriers are only weakly temperature dependent in the supercooled region. They also found that the energy barriers are significantly greater than k_BT, even in the temperature range where MCT can provide useful predictions.

The interpretation of super-Arrhenius behavior in terms of a temperature-dependent entropy or prefactor is lent some support by previous studies of the network properties of the PES.[89] This work revealed that the number of connections between local minima can be very large and may vary between different parts of the landscape.

The (incorrect) KMC behavior contrasts with the Adam–Gibbs picture (Sec. II A), where the free energy barrier to diffusion grows with decreasing inherent structure entropy. If the Adam–Gibbs equation were directly applicable to the present system, we would expect $\Delta E_{KMC}^{\dagger}$ to be close to $\Delta E_{MD}^{\dagger}(T_c)$. Some simulations have reported rearrangement mechanisms involving chainlike clusters in similar LJ systems,[90] which contribute increasingly to diffusion as $T\to T_c$. These processes have not yet been characterized in terms of stationary points of the PES, but we can be confident that our KMC results include such spatial correlations. If these processes were not sampled, one would expect the diffusion constant to be significantly different from that obtained by MD simulations, even as $T\to T_c$, which is not the case.

In Refs. 54 and 55 we noted that the normal-mode frequencies for the BLJ system depend on the potential energy of the minimum.[34] However, this factor is accounted for in both the KMC and MD results, and so cannot be the cause of the discrepancies in the prefactor. Changing connectivity between megabasins and associated sampling problems remains the most likely reason that the KMC results do not replicate the MD results. If this is the case, then it suggests that higher-lying minima are, on average, connected to more minima by kinetically accessible barriers than lower-lying minima are. Sampling of higher-energy minima would then be crucial to the calculation of the diffusion constant. Our current implementation of the KMC algorithm has apparently failed to cope with the Gaussian density of minima at higher energy.

The notion that the temperature dependence of the diffusion constant is controlled by entropy has been discussed before. In particular, the way we interpret the correlation between the dynamics of the system and entropy is similar to Keyes' INM-REM analysis (Sec. II B).[23,24,45] In this model, $\ln f_{dw} \sim S_{\mathrm{IS}}$, where S_{IS} is the inherent structure entropy, extended to include other stationary points as well as minima. This analysis suggests that $D \sim \exp(S_{\mathrm{IS}})$, which is reminiscent of Dzugutov's universal scaling law (Sec. II C).[25,53,91] However, we emphasize that our current interpretation is somewhat speculative, and further work is needed to confirm the source of the discrepancies in the KMC data.

VI. CONCLUSIONS

We now combine the INM-REM, Dzugutov, and inherent structure approaches to suggest an explanation of our KMC results. It appears that in this BLJ system the potential energy barriers relevant for diffusion are similar throughout the region of the PES explored by the supercooled liquid. Our results suggest that the super-Arrhenius behavior observed in MD simulations is due to decreased connectivity in the lower-energy regions of the PES. The most important energy barriers to diffusion are the lowest ones. Theory also suggests that the total number of transition states should scale linearly with the number of local minima.[47] If this result also holds when comparing minima in different energy ranges, then the number of low-barrier pathways between megabasins sampled at a given energy may be roughly proportional to their number. This connectivity contribution is entropic and would probably scale as $\exp(S_{\mathrm{IS}})$, producing the relationship

$$D \sim \exp[S_{\mathrm{IS}}(T)/B - \Delta E^{\dagger}/k_B T], \tag{8}$$

where B is a constant with dimensions of entropy. This result is similar to an equation proposed by Di Marzio and Yang,[1] which employs the potential energy, rather than the energy barrier.

Neglecting the possible temperature dependence of $\Delta E^{\dagger}$, the gradient of an Arrhenius plot for D is given by

$$\frac{d \ln D}{d(1/T)} = -\frac{T^2}{B}\frac{dS_{\mathrm{IS}}(T)}{dT} - \frac{\Delta E^{\dagger}}{k_B}. \tag{9}$$

In the high-temperature limit, where $k_B T \gg \Delta E^{\dagger}$, the entropic term will dominate, and we recover relationships similar to those of Dzugutov[25,53,91] and Keyes and co-workers.[23,24,45] However, as the temperature decreases, we see a departure from these formulations because the energetic term becomes significant. (Dzugutov's relationship uses excess entropy rather than configurational entropy. It has been argued that they are proportional to each other,[37] and in any case for the purposes of this general discussion, we can treat the two approaches as being qualitatively similar.) The connectivity of megabasins on the PES that contributes to diffusion appears to increase as the potential energy increases. However, we again note that further calculations are needed to confirm the source of the discrepancies in the KMC data.

A decrease in the free energy barrier to diffusion below T_g has been observed in trinaphthyl benzene (TNB).[92] In our picture, the entropic contribution to the temperature dependence of transport processes is due to decreasing connectivity between megabasins at low potential energy. At T_g, the liquid is no longer able to relax to lower potential energy regions of the PES on the experimental time scale, and so the observed temperature dependence of S_{IS} will be much weaker. Only the second term in Eq. (9) is then significant, and so the gradient of the Arrhenius plot decreases. A crossover to Arrhenius behavior has recently been observed in longer-time-scale simulations in a BLJ system below T_c (Ref. 93). However, there is no evidence to suggest that the activation energy decreases below T_c, as in TNB below T_g. A complementary analysis of non-Arrhenius behavior, including further experimental results, has recently been provided by Zaman and co-workers.[94]

Our picture of the connectivity between megabasins is probably consistent with the relation $D \sim f_{dw}$. If we interpret the expression for D in Eq. (8) in terms of the accessible connectivity times a Boltzmann factor, then it is not unreasonable that this should be related to the time-averaged sampling of diffusive degrees of freedom. However, a detailed analysis of the relations between existing theories is a topic for future research.

In Ref. 55 we observed that potential energy barriers for ''cage-breaking'' diffusive rearrangements become larger with increasing density. Thus, while these barriers may be similar in both high- and low-lying regions of the PES at constant volume, we expect that at constant pressure, as in most experiments, the potential energy barriers may grow with decreasing temperature as the system becomes denser.

To summarize, we have used the discrepancies between KMC and MD simulations to infer properties of the PES for the 60-atom binary Lennard-Jones system that are difficult to obtain directly. Approaching T_g, there are still diffusive pathways accessible to the system with activation free energies close to the high-temperature limiting value. Hence, in this atomic glass, the potential energy barriers for diffusion do not change very much in different regions of the PES. Instead we tentatively suggest, by a process of elimination, that the connectivity between megabasins, which appears as an entropic prefactor, is related to the inherent structure entropy.

[1] E. A. Di Marzio and A. J. M. Yang, J. Res. Natl. Inst. Stand. Technol. **102**, 135 (1997).
[2] G. S. Fulcher, J. Am. Ceram. Soc. **8**, 339 (1925).
[3] H. Vogel, Z. Phys. **22**, 645 (1921).
[4] G. Tammann and W. Z. Hesse, Z. Anorg. Allg. Chem. **156**, 245 (1926).
[5] F. Stickel, E. W. Fischer, and A. Schönhals, Phys. Rev. Lett. **73**, 2936 (1991).
[6] F. Stickel, F. Kremer, and E. W. Fischer, Physica A **201**, 318 (1993).
[7] C. A. Angell, J. Non-Cryst. Solids **102**, 205 (1988).
[8] M. Paluch, S. J. Rzoska, P. Habdas, and J. Ziolo, J. Phys.: Condens. Matter **8**, 10885 (1996).
[9] M. Paluch, J. Ziolo, and S. J. Rzoska, Phys. Rev. E **56**, 5764 (1997).
[10] C. A. Angell, Science **267**, 1924 (1995).
[11] W. Kauzmann, Chem. Rev. **43**, 219 (1948).
[12] C. A. Angell, J. Non-Cryst. Solids **131–133**, 13 (1991).
[13] J. H. Gibbs and E. A. Di Marzio, J. Chem. Phys. **28**, 373 (1958).
[14] E. A. Di Marzio and J. H. Gibbs, J. Chem. Phys. **28**, 807 (1958).
[15] J. N. Murrell and K. J. Laidler, Trans. Faraday Soc. **64**, 371 (1968).
[16] G. Adam and J. H. Gibbs, J. Chem. Phys. **43**, 139 (1965).
[17] P. G. Wolynes, Proc. Natl. Acad. Sci. U.S.A. **94**, 6170 (1997).
[18] G. Seeley and T. Keyes, J. Chem. Phys. **91**, 5581 (1989).
[19] T. Keyes, J. Chem. Phys. **103**, 9810 (1995).
[20] B. Madan and T. Keyes, J. Chem. Phys. **98**, 3342 (1993).
[21] T. Keyes, J. Phys. Chem. A **101**, 2921 (1997).
[22] T. Keyes, J. Chem. Phys. **101**, 5081 (1994).
[23] T. Keyes, J. Chowdhary, and J. Kim, Phys. Rev. E **66**, 051110 (2002).
[24] T. Keyes, Phys. Rev. E **62**, 7905 (2000).
[25] M. Dzugutov, Nature (London) **381**, 137 (1996).
[26] P. Richert, Geochim. Cosmochim. Acta **48**, 47 (1984).
[27] G. W. Scherer, J. Am. Ceram. Soc. **67**, 504 (1984).
[28] P. Richert and Y. Bottinga, Rev. Geophys. **24**, 1 (1986).
[29] I. M. Hodge, Macromolecules **20**, 2897 (1987).
[30] Y. Bottinga, P. Richert, and A. Sipp, Am. Mineral. **80**, 305 (1995).
[31] S. Takahara, O. Yamamuro, and T. Matsuo, J. Phys. Chem. **99**, 9589 (1995).
[32] S. Kamath, R. H. Colby, S. K. Kumar, and J. Baschnagel, J. Chem. Phys. **116**, 865 (2002).
[33] A. Scala, F. W. Starr, E. La Nave, F. Sciortino, and H. E. Stanley, Nature (London) **406**, 166 (2000).
[34] S. Sastry, Nature (London) **409**, 164 (2001).
[35] I. Saika-Volvod, P. H. Poole, and F. Sciortino, Nature (London) **412**, 514 (2001).
[36] R. J. Speedy, J. Chem. Phys. **114**, 9069 (2001).
[37] L.-M. Martinez and C. A. Angell, Nature (London) **410**, 663 (2001).
[38] E. L. Nave, H. E. Stanley, and F. Sciortino, Phys. Rev. Lett. **88**, 035501 (2002).
[39] S. Mossa, E. L. Nave, H. E. Stanley, C. Donati, F. Sciortino, and P. Tartaglia, Phys. Rev. E **65**, 041205 (2002).
[40] B. Derrida, Phys. Rev. Lett. **45**, 79 (1980).
[41] J. D. Ferry, J. Am. Chem. Soc. **72**, 3746 (1950).
[42] R. Zwanzig, J. Chem. Phys. **79**, 4507 (1983).
[43] J. Chowdhary and T. Keyes, Physica A **314**, 575 (2002).
[44] J. Chowdhary and T. Keyes, Phys. Rev. E **65**, 026125 (2002).
[45] U. Zürcher and T. Keyes, Phys. Rev. E **60**, 2065 (1999).
[46] E. LaNave, A. Scala, F. W. Starr, F. Sciortino, and H. E. Stanley, Phys. Rev. Lett. **84**, 4605 (2000).
[47] J. P. K. Doye and D. J. Wales, J. Chem. Phys. **116**, 3777 (2002).
[48] D. J. Wales and J. P. K. Doye, J. Chem. Phys. **119**, 12409 (2003).
[49] S. Chapman and T. G. Cowling, *The Mathematical Theory of Nonuniform Gases* (Cambridge University Press, Cambridge, England, 1939).
[50] J.-P. Hansen and I. R. McDonald, *Theory of Simple Liquids* (Academic, New York, 1986).
[51] H. J. Raveche, J. Chem. Phys. **35**, 2242 (1971).
[52] J. J. Hoyt, M. Asta, and B. Sadigh, Phys. Rev. Lett. **85**, 594 (2000).
[53] M. Dzugutov, Phys. Rev. E **65**, 032501 (2002).
[54] T. F. Middleton and D. J. Wales, Phys. Rev. B **64**, 024205 (2001).
[55] T. F. Middleton and D. J. Wales, J. Chem. Phys. **118**, 4583 (2003).
[56] J. Hernández-Rojas and D. J. Wales, in *The Monte Carlo Method in the Physical Sciences*, edited by J. E. Gubernatis (AIP, Melville, NY, 2003), pp. 334–343.
[57] K. A. Fichthorn and W. H. Weinberg, J. Chem. Phys. **95**, 1090 (1991).
[58] A. B. Bortz, M. H. Kalos, and J. L. Leibowitz, J. Comput. Phys. **17**, 10 (1975).
[59] O. K. Rice and H. C. Ramsperger, J. Am. Chem. Soc. **49**, 1617 (1927).
[60] L. S. Kassel, J. Phys. Chem. **32**, 225 (1928).
[61] A. Marcus and O. K. Rice, J. Phys. Colloid Chem. **55**, 894 (1951).
[62] D. J. Wales, J. P. K. Doye, M. A. Miller, P. N. Mortenson, and T. R. Walsh, Adv. Chem. Phys. **115**, 1 (2000).
[63] D. J. Wales, *Energy Landscapes* (Cambridge University Press, Cambridge, England, 2003).
[64] J. Horbach, W. Kob, and K. Binder, J. Phys. Chem. B **103**, 4104 (1999).
[65] K. Broderix, K. K. Bhattacharya, A. Cavagna, A. Zippelius, and I. Giardina, Phys. Rev. Lett. **85**, 5360 (2000).
[66] H. C. Kang and W. H. Weinberg, J. Chem. Phys. **90**, 2824 (1988).
[67] L. A. Ray and R. C. Baetzold, J. Chem. Phys. **93**, 2871 (1990).
[68] M. I. Larsson, Phys. Rev. B **64**, 115 428 (2001).
[69] F. M. Bulnes, V. D. Pereyra, and J. L. Riccardo, Phys. Rev. E **58**, 86 (1998).
[70] G. Henkelman and H. Jónsson, J. Chem. Phys. **115**, 9657 (2001).
[71] R. Q. Snurr, A. T. Bell, and D. N. Theodorou, J. Phys. Chem. **98**, 11 948 (1994).
[72] W. Kob and H. C. Andersen, Phys. Rev. Lett. **73**, 1376 (1994).
[73] W. Kob and H. C. Andersen, Phys. Rev. E **51**, 4626 (1995).
[74] W. Kob and H. C. Andersen, Phys. Rev. E **52**, 4134 (1995).
[75] S. Büchner and A. Heuer, Phys. Rev. Lett. **84**, 2168 (2000).
[76] T. Keyes and J. Chowdhary, Phys. Rev. E **64**, 032201 (2001).
[77] R. A. Denny, D. R. Reichman, and J. P. Bouchaud, Phys. Rev. Lett. **90**, 025503 (2003).
[78] L. Berthier and J. P. Garrahan, J. Chem. Phys. **119**, 4367 (2003).
[79] T. F. Middleton, Ph.D. thesis, Cambridge University, 2003.
[80] D. J. Wales, Mol. Phys. **100**, 3285 (2002).
[81] H. Jónsson, G. Mills, and K. W. Jacobsen, in *Classical and Quantum Dynamics in Condensed Phase Simulations*, edited by B. J. Berne, G. Ciccotti, and D. F. Coker (World Scientific, Singapore, 1998).
[82] J. E. Lennard-Jones, Proc. R. Soc. London, Ser. A **106**, 463 (1924).
[83] S. D. Stoddard and J. Ford, Phys. Rev. A **8**, 1504 (1973).
[84] M. Allen and D. J. Tildesley, *Computer Simulation of Liquids* (Clarendon, Oxford, 1987).
[85] S. Sastry, P. G. Debenedetti, and F. H. Stillinger, Nature (London) **393**, 554 (1998).
[86] A. Mukherjee, S. Bhattacharyya, and B. Bagchi, J. Chem. Phys. **116**, 4577 (2002).
[87] B. Doliwa and A. Heuer, Phys. Rev. E **67**, 031506 (2003).
[88] B. Doliwa and A. Heuer, J. Phys.: Condens. Matter **15**, S849 (2003).
[89] J. P. K. Doye, Phys. Rev. Lett. **88**, 238 701 (2002).
[90] C. Donati, S. C. Glotzer, P. H. Poole, W. Kob, and S. J. Plimpton, Phys. Rev. E **60**, 3107 (1999).
[91] M. Dzugutov, J. Phys.: Condens. Matter **11**, A253 (1999).
[92] D. Plazek, J. Chem. Phys. **49**, 3678 (1968).
[93] S. S. Ashwin and S. Sastry, J. Phys.: Condens. Matter **15**, S1253 (2003).
[94] M. H. Zaman, T. R. Sosnick, and R. S. Berry, Phys. Chem. Chem. Phys. **5**, 2589 (2003).